

MoE-TinyMed: Mixture of Experts for Tiny Medical Large Vision-Language Models

Songtao Jiang^{*1}, Tuo Zheng^{*1}, Yan Zhang², Yeying Jin² and Zuozhu Liu¹

¹Zhejiang University

²National University of Singapore

Abstract

Mixture of Expert Tuning (MoE-Tuning) has effectively enhanced the performance of general MLLMs with fewer parameters, yet its application in resource-limited medical settings has not been fully explored. To address this gap, we developed MoE-TinyMed, a model tailored for medical applications that significantly lowers parameter demands. In evaluations on the VQA-RAD, SLAKE, and Path-VQA datasets, MoE-TinyMed outperformed LLaVA-Med in all Med-VQA closed settings with just 3.6B parameters. Additionally, a streamlined version with 2B parameters surpassed LLaVA-Med’s performance in PathVQA, showcasing its effectiveness in resource-limited healthcare settings. Our code released on <https://github.com/jiangsongtao/TinyMed>.

1 Introduction

In the AI for Healthcare domain, creating systems with human-like multimodal understanding is essential for managing complex medical data (Miao et al., 2022; Goyal et al., 2016; de Faria et al., 2023; Antol et al., 2015). Despite this, current Multimodal Large Language Models (MLLMs) such as LLaVA (Liu et al., 2024), MiniGPT4-V2 (Chen et al., 2023), CogVLM (Wang et al., 2023), and MoE-LLaVA (Lin et al., 2024) often fall short in healthcare-specific tasks like Medical Visual Question Answering (Med-VQA) due to their reliance on general, diverse datasets. The need for specialized medical data, the prevalence of grayscale imaging, and training set disparities demand customized training approaches. Models like Med-Flamingo (Moor et al., 2023), Med-PaLM M (Singhal et al., 2023), and LLaVA-Med (Li et al., 2024) demonstrate the effectiveness of medical-specific training, with LLaVA-Med using instruction-tuning to reach top performance in Med-VQA. Yet, the extensive parameter activation required by traditional

^{*}Equal contribution

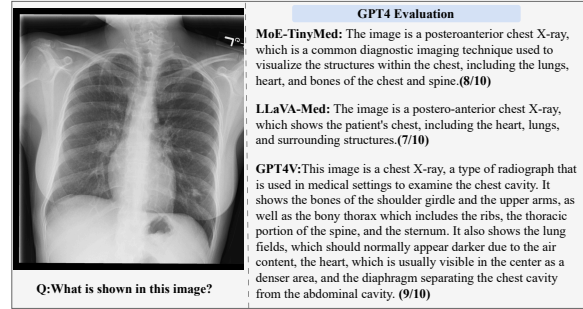


Figure 1: A Med-VQA example demonstrating our model’s capability to surpass the performance of LLaVA-Med with 7B activated parameters, using only 2B activated parameters. Detailed evaluation specifics are shown in Supplementary Figure 6.

models incurs high computational costs, highlighting the necessity for more cost-efficiency models that meet the operational and economic needs of medical AI without sacrificing much performance.

Inspired by Mixture of Expert LLaVA (MoE-LLaVA)’s use of a sparse, MoE-based architecture, we developed MoE-TinyMed for the medical sector. This model significantly cuts parameter count while matching or exceeding the capabilities of larger 7B models, making it ideal for resource-limited settings. In evaluations on the VQA-RAD (Lau et al., 2018), SLAKE (Liu et al., 2021), and Path-VQA (He et al., 2020) datasets, MoE-TinyMed, building on the Phi2 architecture, outperformed LLaVA-Med in closed Med-VQA settings with just 3.6B parameters. A more compact version with only 2B activated parameters trained on StableLM further surpassed LLaVA-Med’s performance in PathVQA and achieved comparable performance on both SLAKE and VQA-RAD datasets, showcasing cost-effective MLLMs’ potential in healthcare.

2 Methods

Following the MoE-LLaVA framework (Lin et al., 2024), we structured the MoE-TinyMed model

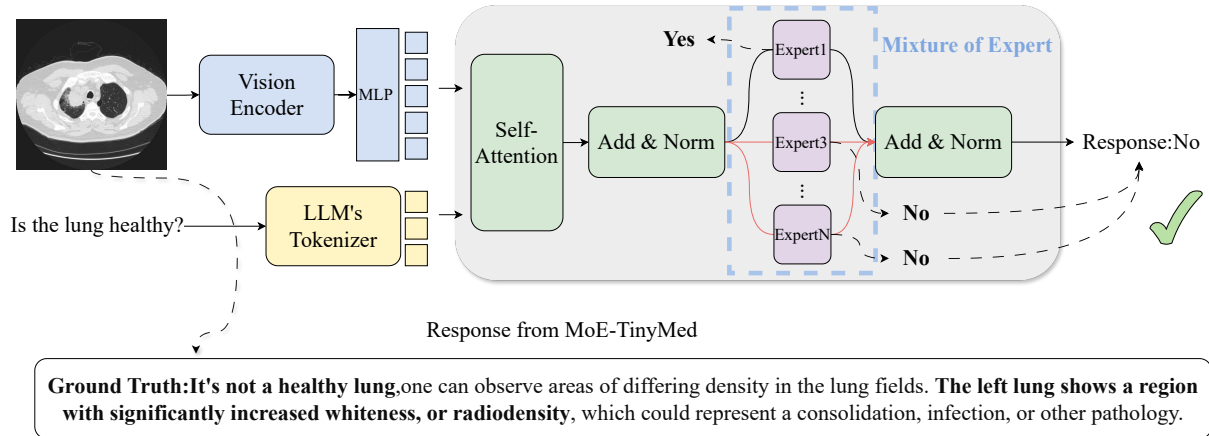


Figure 2: Model Framework: This diagram depicts the MoE-TinyMed architecture, which processes medical images and corresponding questions as inputs. A sparse Feedforward Network (FFN) equipped with a router dynamically selects the top-k most relevant experts for answering the question. Each expert contributes to the prediction of the next token based on their specialized knowledge, integrating these predictions to select the most probable next token, ultimately forming the model’s output response.

Table 1: Summary of Data Utilized Across Training Stages.

Stage	Data Source	Sample
Stage 1	llava_med_alignment_500k	500K
Stage 2	instruct_60k_inline_mention	60k
Stage 3	VQA-RAD, SLAKE, Path-VQA	27k

training into three stages, illustrated in Figure 1. **Stage 1: Medical Multimodal Feature Alignment** involves using a Multilayer Perceptron (MLP) to transform medical image patches into tokens combined with text tokens, setting the groundwork for the model’s initial understanding of multimodal relationships. **Stage 2: Medical Multimodal Instruction Tuning** freezes the visual encoder and refines the neural network to enhance generalization across various medical imaging modalities. **Stage 3: Mixture of Medical Experts Finetuning** integrates MoE-tuning to improve performance on specialized tasks like medical visual question answering, leveraging precise expertise for complex medical queries.

3 Experiments

3.1 Datasets

During the pretraining phase, our MoE-TinyMed model utilized 500k image-text pairs from PMC-15M as provided by LLaVA-Med (Li et al., 2024). For instruction tuning, we employed datasets encompassing five primary imaging modalities—CXR, CT, MRI, histopathology, and gross pathology—outlined in LLaVA-Med (Li et al.,

2024), and enhanced our model’s expertise with additional data from trainsets of VQA-RAD (Lau et al., 2018), SLAKE (Liu et al., 2021), and PathVQA (He et al., 2020) for downstream tasks. This integration of datasets is summarized in Table 1. For evaluation, testsets of these biomedical VQA datasets were used, with detailed examples of MoE-TinyMed’s responses, show in Figure 3 and Supplementary Figure 7.

We adopted a consistent approach to evaluation across tasks: accuracy was used for closed-set questions and recall for open-set questions, maintaining alignment with LLaVA-Med’s methodology for fair and unbiased comparison. Additionally, in zero-shot settings, our models were not fine-tuned on any specific VQA dataset, ensuring rigorous and impartial benchmarking standards.

3.2 Results

Zero Shot Performance: In the zero-shot setting, without fine-tuning on medical VQA data, TinyMoE-Med, particularly the (Phi2-2.7B×4:3.6B) variant, outperformed LLaVA-Med in open settings on the VQA-RAD and SLAKE datasets. The TinyMoE-Med (Phi2-2.7B×4:3.6B) model achieved an open question accuracy of 61.75% in VQA-RAD and 56.97% in SLAKE, exceeding LLaVA-Med’s 60.16% and 47.60%, respectively. This superior zero-shot performance demonstrates TinyMoE-Med’s capability to capture and interpret medical domain-specific nuances effectively. Additionally, the (StableLM-1.6B×4:2.0B) variant also displayed strong perfor-

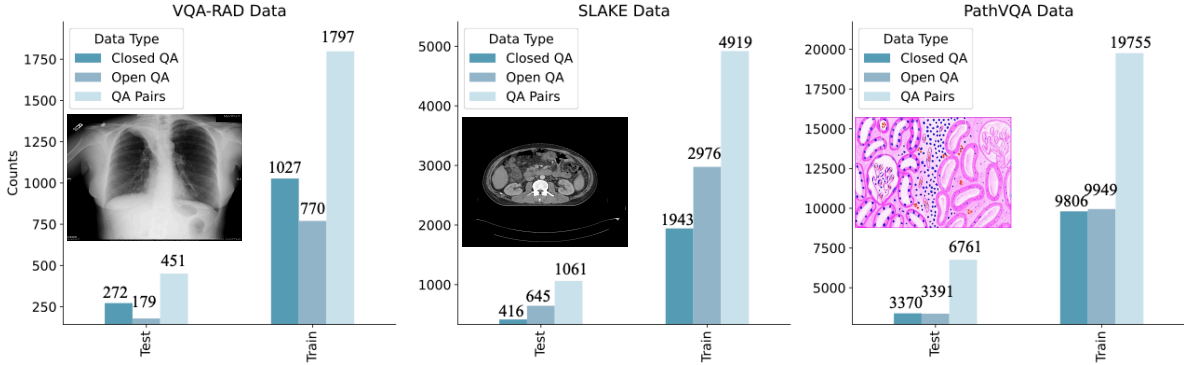


Figure 3: This figure displays Medical VQA cases from VQA-RAD, SLAKE, and Path-VQA datasets, illustrating the distribution of Open and Closed settings within each dataset. For more cases, see Supplementary Figure 7.

Method	VQA-RAD		SLAKE		PathVQA	
	Open	Closed	Open	Closed	Open	Closed
<i>Supervised finetuning results with our own experiment runs</i>						
LLaVA	50.00	65.07	78.18	63.22	7.74	63.20
LLaVA-Med (LLama7B)	61.52	84.19	83.08	85.34	37.95	91.21
LLaVA-Med (Vicuna7B)	64.39	81.98	84.71	83.17	38.87	91.65
TinyMoE-Med (Phi2-2.7B×4:3.6B)	52.55	84.56	85.27	86.78	33.83	91.98
TinyMoE-Med (StableLM-1.6B×4:2.0B)	47.26	83.82	82.28	84.86	34.07	91.83
<i>Zero-shot results</i>						
LLaVA-Med (LLama7B)	36.23	60.16	41.72	47.60	10.86	59.75
TinyMoE-Med (Phi2-2.7B×4:3.6B)	36.73	61.75	43.93	56.97	6.94	61.46
TinyMoE-Med (StableLM-1.6B×4:2.0B)	28.02	66.91	40.63	52.64	9.40	69.09
<i>Representative & SoTA methods with numbers reported in the literature</i>						
VL Encoder-Decoder (Bazi et al., 2023)	-	82.47	-	-	-	85.61
Q2ATransformer (Liu et al., 2023)	-	81.20	-	-	54.85	88.85
Prefix T. Medical LM (van Sonsbeek et al., 2023)	-	-	-	82.01	-	87.00
PubMedCLIP (Eslami et al., 2023)	-	80.00	-	82.50	-	-
BiomedCLIP (Zhang et al., 2023)	-	79.80	-	89.70	-	-
M2I2 (Li et al., 2022)	-	83.50	-	91.10	-	88.00

Table 2: This table contrasts our methods with existing state-of-the-art approaches in a supervised setting. It highlights that for open-ended questions, conventional methods may overstate their adaptability by treating the problem as a classification task with predefined answers. This approach could lead to an inflated sense of generalizability, especially in datasets where the answers in the test set are often seen during training.

mance, achieving 69.09% in PathVQA’s open questions, proving the model’s versatility and potential in handling diverse medical imaging challenges without domain-specific training.

Comparison with SoTA Methods: The MoE-Tuning technique places the TinyMoE-Med (Phi2-2.7B×4:3.6B) model at the forefront of state-of-the-art performance in closed settings of VQA-RAD and PathVQA. This model surpasses the benchmarks of LLaVA-Med trained on LLaMA-7B and Vicuna-7B architectures with fewer parameters, showing incremental improvements of 0.37% in VQA-RAD, 1.44% in SLAKE, and 0.33% in PathVQA. The consistent excellence across all tested Med-VQA datasets demonstrates the effectiveness and efficiency of our approach. The lighter TinyMoE-Med (StableLM-1.6B×4:2.0B) variant similarly delivers impressive results, emphasizing

our models’ ability to accurately interpret complex medical visuals while enhancing cost-efficiency.

Ablation of MoE-Tuning To assess the benefits of MoE-Tuning over traditional Supervised Fine-Tuning (SFT), we conducted an ablation study comparing their effects during the third training phase of the Phi2.7B model. The comparison across three Med-VQA datasets, detailed in Table 3, despite the only difference between the two models being the method of training in the third stage, the results clearly demonstrate that MoE-Tuning contributes to noticeable performance improvements. This finding underscores the effectiveness of MoE-Tuning in enhancing model capabilities.

Routing of Medical Experts Analysis from Figures 4 and 5 clearly highlights the strategic roles of experts across MoE layers. Specific experts dominate different layers (Layer 1 to Layer 8), indi-

Method	Configurations				VQA-RAD		SLAKE		PathVQA	
	S1	S2	SFT	MoE Tuning	Open	Closed	Open	Closed	Open	Closed
A	✓	✓	✓		49.89	83.35	83.71	86.14	32.11	91.17
B	✓	✓		✓	52.55 (+2.66)	84.56 (+1.21)	85.27 (+1.56)	86.78 (+0.64)	33.83 (+1.72)	91.98 (+0.81)

Table 3: Performance comparison of two training methods across different datasets with detailed configurations and performance gains.

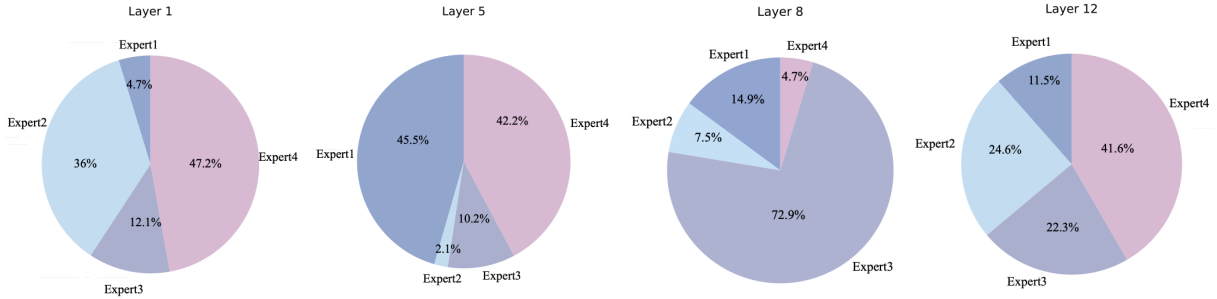


Figure 4: This figure illustrates the activation proportions of each expert within four sequentially selected MoE layers, showcasing the dynamic engagement of experts across the layers.

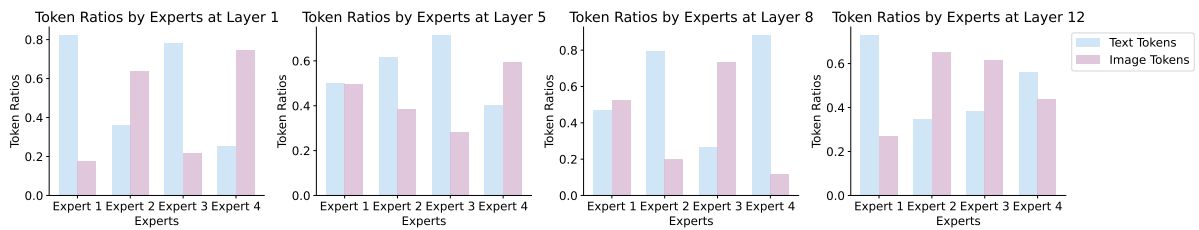


Figure 5: This figure displays the modal proportions handled by each expert during activation across four MoE layers selected sequentially, highlighting how different modalities are processed by individual experts in each layer.

cating specialized functions at particular stages of processing. For instance, Expert 2 is most active in Layer 1, while Expert 4 leads in Layers 1 and 5, and Expert 3 dominates Layer 8. By the final Layer 12, expert contributions equilibrate, illustrating an effective integration of learned features, transitioning from early specialized processing to later unified synthesis. Figure 5 further shows that experts handle distinct modalities, with Expert 1 focusing on textual and Expert 2 on image tokens, ensuring balanced multimodal processing and effectively demonstrating the synergy of MoE-Tuning in managing diverse data types efficiently.

4 Related Work

The advancement of Multimodal Large Language Models (MLLMs) such as Med-Flamingo (Moor et al., 2023), Med-PaLM M (Singhal et al., 2023), and LLaVA-Med (Li et al., 2024) marks significant progress in integrating AI with medical diagnostics and patient care, inspired by general AI developments like ChatGPT (OpenAI, 2022) and GPT-4 (OpenAI, 2023). These models enhance ar-

eas from few-shot learning in medical contexts to boosting medical question answering and conversational AI, demonstrating the transformative impact of specialized MLLMs on healthcare. Additionally, biomedical chatbots such as ChatDoctor (Yunxiang et al., 2023) and Visual Med-Alpaca showcase the benefits of domain-specific fine-tuning. Concurrently, the Mixture of Experts (MoE) strategy (Jacobs et al., 1991; Eigen et al., 2013), which integrates specialized "experts" into a unified architecture and reduces interference through efficient token routing (Fedus et al., 2022; Lepikhin et al., 2020; Shazeer et al., 2017), supports scaling smaller models to match the performance of larger counterparts (Jiang et al.). Successfully implemented in models like MoE-LLaVA (Lin et al., 2024) and SPHINX-X (Gao et al., 2024), this approach has yet to be fully explored in resource-constrained hospital settings, identifying a vital gap in applying cost-efficient MoE-tuned MLLMs for clinical purposes. This underscores the need for further research and development in this area.

5 Discussion and Limitations

Our work primarily sought to develop a smaller, more cost-efficient Multimodal Large Language Model (MLLM) for the medical field, diverging from the current trend focused on creating larger and more robust models. We posit that in practical applications, especially in resource-constrained environments like mobile devices, smaller models could be more advantageous. This approach not only addresses the practical limitations of deploying large-scale models in routine clinical settings but also explores the feasibility of using leaner models without compromising on performance, fostering broader accessibility and application.

However, our approach faces several limitations. First, there is a notable scarcity of training data in the medical domain, largely due to the sensitivity and privacy concerns associated with medical data. Generating synthetic data through methods like those used for GPT-4V can be problematic in this context, and many datasets require labor-intensive manual annotations by medical professionals. This is both costly and limits the scalability of data generation efforts. As illustrated in Supplementary Figure 8, our model occasionally fails, particularly with more complex open-ended questions that demand precise medical knowledge.

Furthermore, the inherent requirement for medical applications to provide trustworthy explanations and confidence scores poses another challenge. Ensuring that the model outputs are not only accurate but also accompanied by reliable justifications is crucial, especially in a field where decisions have significant health implications. This necessity heightens the importance of building a trustworthy MLLM that can articulate its reasoning processes clearly and provide confidence levels, thereby enhancing the reliability and safety of AI applications in healthcare.

Acknowledgments

References

Stanislaw Antol, Aishwarya Agrawal, Jiasen Lu, Margaret Mitchell, Dhruv Batra, C Lawrence Zitnick, and Devi Parikh. 2015. Vqa: Visual question answering. In *Proceedings of the IEEE international conference on computer vision*, pages 2425–2433.

Yakoub Bazi, Mohamad Mahmoud Al Rahhal, Laila Bashmal, and Mansour Zuair. 2023. Vision-language model for visual question answering in medical imagery. *Bioengineering*.

Jun Chen, Deyao Zhu, Xiaoqian Shen, Xiang Li, Zechun Liu, Pengchuan Zhang, Raghuraman Krishnamoorthi, Vikas Chandra, Yunyang Xiong, and Mohamed Elhoseiny. 2023. Minigpt-v2: large language model as a unified interface for vision-language multi-task learning. *arXiv preprint arXiv:2310.09478*.

Ana Cláudia Akemi Matsuki de Faria, Felype de Castro Bastos, José Victor Nogueira Alves da Silva, Vitor Lopes Fabris, Valeska de Sousa Uchoa, Décio Gonçalves de Aguiar Neto, and Claudio Filipi Goncalves dos Santos. 2023. Visual question answering: A survey on techniques and common trends in recent literature. *arXiv preprint arXiv:2305.11033*.

David Eigen, Marc’Aurelio Ranzato, and Ilya Sutskever. 2013. Learning factored representations in a deep mixture of experts. *arXiv preprint arXiv:1312.4314*.

Sedigheh Eslami, Christoph Meinel, and Gerard De Melo. 2023. Pubmedclip: How much does clip benefit visual question answering in the medical domain? In *Findings of the Association for Computational Linguistics: EACL 2023*, pages 1151–1163.

William Fedus, Barret Zoph, and Noam Shazeer. 2022. Switch transformers: Scaling to trillion parameter models with simple and efficient sparsity. *Journal of Machine Learning Research*, 23(120):1–39.

Peng Gao, Renrui Zhang, Chris Liu, Longtian Qiu, Siyuan Huang, Weifeng Lin, Shitian Zhao, Shijie Geng, Ziyi Lin, Peng Jin, et al. 2024. Sphinx-x: Scaling data and parameters for a family of multi-modal large language models. *arXiv preprint arXiv:2402.05935*.

Yash Goyal, Akrit Mohapatra, Devi Parikh, and Dhruv Batra. 2016. Towards transparent ai systems: Interpreting visual question answering models. *arXiv preprint arXiv:1608.08974*.

Xuehai He, Yichen Zhang, Luntian Mou, Eric Xing, and Pengtao Xie. 2020. Pathvqa: 30000+ questions for medical visual question answering. *arXiv preprint arXiv:2003.10286*.

Robert A Jacobs, Michael I Jordan, Steven J Nowlan, and Geoffrey E Hinton. 1991. Adaptive mixtures of local experts. *Neural computation*, 3(1):79–87.

Albert Q Jiang, Alexandre Sablayrolles, Antoine Roux, Arthur Mensch, Blanche Savary, Chris Bamford, and Devendra Singh Chaplot. Diego de las casas, emma bou hanna, florian bressand, et al. 2024. mixtral of experts. *arXiv preprint arXiv:2401.04088*.

Jason J Lau, Soumya Gayen, Asma Ben Abacha, and Dina Demner-Fushman. 2018. A dataset of clinically generated visual questions and answers about radiology images. *Scientific data*, 5(1):1–10.

Dmitry Lepikhin, HyoukJoong Lee, Yuanzhong Xu, Dehao Chen, Orhan Firat, Yanping Huang, Maxim Krikun, Noam Shazeer, and Zhifeng Chen. 2020.

- Gshard: Scaling giant models with conditional computation and automatic sharding. *arXiv preprint arXiv:2006.16668*.
- Chunyuan Li, Cliff Wong, Sheng Zhang, Naoto Usuyama, Haotian Liu, Jianwei Yang, Tristan Naumann, Hoifung Poon, and Jianfeng Gao. 2024. Llavamed: Training a large language-and-vision assistant for biomedicine in one day. *Advances in Neural Information Processing Systems*, 36.
- Pengfei Li, Gang Liu, Lin Tan, Jinying Liao, and Shenjun Zhong. 2022. Self-supervised vision-language pretraining for medical visual question answering. *arXiv preprint arXiv:2211.13594*.
- Bin Lin, Zhenyu Tang, Yang Ye, Jiayi Cui, Bin Zhu, Peng Jin, Junwu Zhang, Munan Ning, and Li Yuan. 2024. Moe-llava: Mixture of experts for large vision-language models. *arXiv preprint arXiv:2401.15947*.
- Bo Liu, Li-Ming Zhan, Li Xu, Lin Ma, Yan Yang, and Xiao-Ming Wu. 2021. Slake: A semantically-labeled knowledge-enhanced dataset for medical visual question answering. In *2021 IEEE 18th International Symposium on Biomedical Imaging (ISBI)*, pages 1650–1654. IEEE.
- Haotian Liu, Chunyuan Li, Qingyang Wu, and Yong Jae Lee. 2024. Visual instruction tuning. *Advances in neural information processing systems*, 36.
- Yunyi Liu, Zhanyu Wang, Dong Xu, and Luping Zhou. 2023. Q2atransformer: Improving medical vqa via an answer querying decoder. *arXiv preprint arXiv:2304.01611*.
- Yalin Miao, Shuyun He, WenFang Cheng, Guodong Li, and Meng Tong. 2022. Research on visual question answering based on dynamic memory network model of multiple attention mechanisms. *Scientific Reports*, 12(1):16758.
- Michael Moor, Qian Huang, Shirley Wu, Michihiro Yasunaga, Yash Dalmia, Jure Leskovec, Cyril Zakkas, Eduardo Pontes Reis, and Pranav Rajpurkar. 2023. Med-flamingo: a multimodal medical few-shot learner. In *Machine Learning for Health (ML4H)*, pages 353–367. PMLR.
- OpenAI. 2022. ChatGPT. <https://openai.com/blog/chatgpt/>.
- OpenAI. 2023. GPT-4 technical report. <https://arxiv.org/abs/2303.08774>. *Preprint*, arXiv:2303.08774.
- Noam Shazeer, Azalia Mirhoseini, Krzysztof Maziarz, Andy Davis, Quoc Le, Geoffrey Hinton, and Jeff Dean. 2017. Outrageously large neural networks: The sparsely-gated mixture-of-experts layer. *arXiv preprint arXiv:1701.06538*.
- Karan Singh, Tao Tu, Juraj Gottweis, Rory Sayres, Ellery Wulczyn, Le Hou, Kevin Clark, Stephen Pfohl, Heather Cole-Lewis, Darlene Neal, et al. 2023. Towards expert-level medical question answering with large language models. *arXiv preprint arXiv:2305.09617*.
- Tom van Sonsbeek, Mohammad Mahdi Derakhshani, Ivona Najdenkoska, Cees GM Snoek, and Marcel Worring. 2023. Open-ended medical visual question answering through prefix tuning of language models. *arXiv preprint arXiv:2303.05977*.
- Weihan Wang, Qingsong Lv, Wenmeng Yu, Wenyi Hong, Ji Qi, Yan Wang, Junhui Ji, Zhuoyi Yang, Lei Zhao, Xixuan Song, et al. 2023. CogVLM: Visual expert for pretrained language models. *arXiv preprint arXiv:2311.03079*.
- Li Yunxiang, Li Zihan, Zhang Kai, Dan Ruilong, and Zhang You. 2023. Chatdoctor: A medical chat model fine-tuned on llama model using medical domain knowledge. *arXiv preprint arXiv:2303.14070*.
- Sheng Zhang, Yanbo Xu, Naoto Usuyama, Jaspreet Bagga, Robert Tinn, Sam Preston, Rajesh Rao, Mu Wei, Naveen Valluri, Cliff Wong, et al. 2023. Large-scale domain-specific pretraining for biomedical vision-language processing. *arXiv preprint arXiv:2303.00915*.

A Appendix

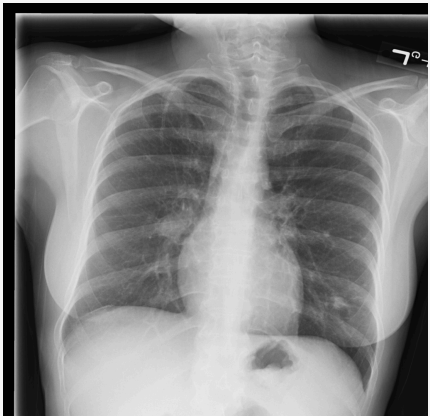
	<div data-bbox="726 604 1356 694" style="text-align: center; background-color: #e0f0ff; border-radius: 10px; padding: 5px;">GPT4 Evaluation</div> <div data-bbox="702 716 1380 828" style="background-color: #e0f0ff; border-radius: 10px; padding: 10px;"> <p>Assuming you are a doctor, please rate the following three answers about this medical picture from 0 to 10, and tell me why.</p> </div> <p>From the perspective of a medical professional:</p> <ol style="list-style-type: none"> <li data-bbox="702 907 1356 1041">1. This explanation is detailed and accurate, so I'd give it an 8 out of 10. It mentions the specific posteroanterior view, which is essential for proper interpretation of a chest X-ray. It also lists the structures that are typically assessed with this imaging technique, though it does not provide much detail about what might be diagnosed with this information. <li data-bbox="702 1097 1388 1209">2. I would rate this explanation a 7 out of 10. While it correctly identifies the type of chest X-ray, it does not offer any additional details beyond what the first explanation provides. The term "surrounding structures" is somewhat vague and could be expanded upon for clarity. <li data-bbox="702 1243 1396 1422">3. This response gets a 9 out of 10. It offers an extensive overview of the anatomy visible on a chest X-ray, noting the appearance of normal lung fields, the positioning of the heart, and the visibility of the diaphragm. It goes further to explain the clinical utility of a chest X-ray, detailing various conditions it can help diagnose. This level of detail is very informative and has significant educational value for understanding both the anatomy and the clinical reasoning behind the use of chest X-rays. <p>The ratings are based on the depth and utility of the information provided. The third response is rated highest because it provides a thorough explanation that could enhance understanding in a clinical education context and assist in patient care decisions.</p>
<p>Q: What is shown in this image?</p> <p>MoE-TinyMed: The image is a posteroanterior chest X-ray, which is a common diagnostic imaging technique used to visualize the structures within the chest, including the lungs, heart, and bones of the chest and spine.</p> <p>LLaVA-Med: The image is a postero-anterior chest X-ray, which shows the patient's chest, including the heart, lungs, and surrounding structures.</p> <p>GPT4V: This image is a chest X-ray, a type of radiograph that is used in medical settings to examine the chest cavity. It shows the bones of the shoulder girdle and the upper arms, as well as the bony thorax which includes the ribs, the thoracic portion of the spine, and the sternum. It also shows the lung fields, which should normally appear darker due to the air content, the heart, which is usually visible in the center as a denser area, and the diaphragm separating the chest cavity from the abdominal cavity.</p>	

Figure 6: An example showcasing our method's ability to answer medical imaging questions with performance nearing or even surpassing that of LLaVA-Med under GPT-4V evaluation.


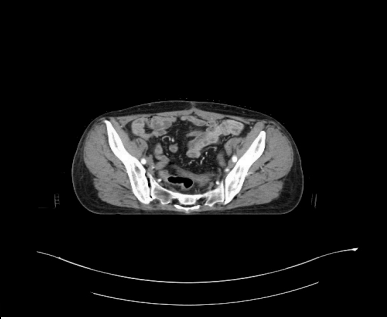


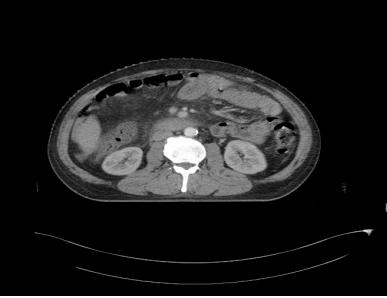
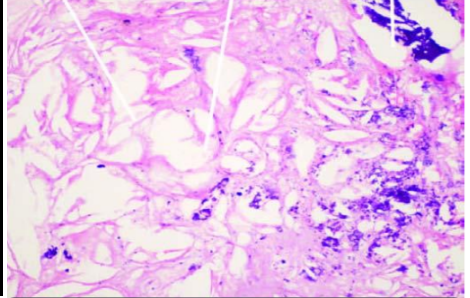
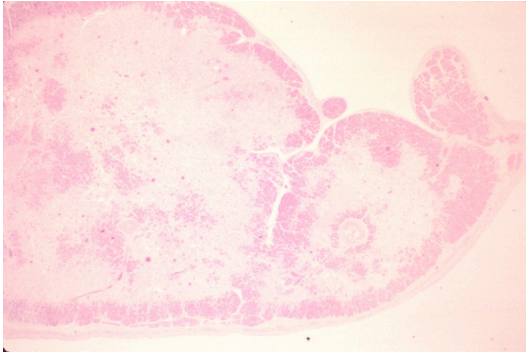
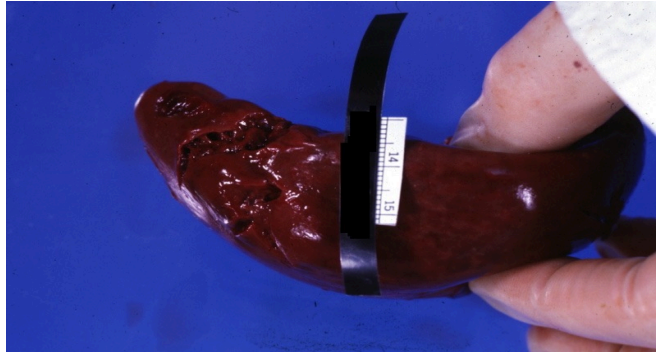
Case from RAD-VQA	Case from SLAKE	Case from Path-VQA
		
<p>Q:The image is taken in what plane? A:Axial</p>	<p>Q:Which is smaller in this image, colon or small bowel? A:Colon</p>	<p>Q:Does typical tuberculous exudate show obvious lesion? A:No</p>
		
<p>Q:Is there air outside the bowel walls? A:No</p>	<p>Q:What is the shape of spinal cord in this image? A:Circular</p>	<p>Q:Is there narrowing of the lumen of coronary due to fully developed atheromatous plaque which has dystrophic calcification in its core? A:No</p>

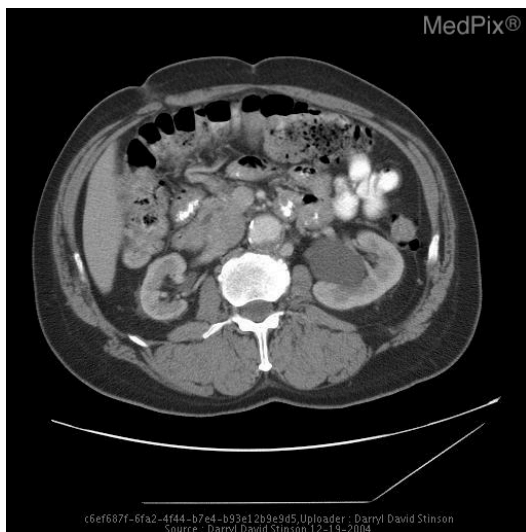
Figure 7: More Medical VQA cases from VQA-RAD, SLAKE, and Path-VQA. our MoE-TinyMed generates expected responses for medical image queries.



Q: What is present?
 A: endocrine
 GT: cardiovascular



Q: What done external view of lacerations of capsule done during?
 A: dissection
 GT: done surgical procedure



Q: What are the hyperdense lesions noted at the edges of the aorta?
 A: Calcifications
 GT: Calcified atherosclerosis



Q: What structures are involved?
 A: basal ganglia, cerebellum, cerebral cortex
 GT: Caudate, putamen, left parietal

Figure 8: Incorrect cases: Med-VQA examples in OPEN setting requiring precise and specialized medical knowledge.